Braking Control Method for Front-and-Rear-Wheel-Independent-Drive-Type Electric Vehicles (FRID EVs) on Low-Friction-Coefficient Roads

Nobuyoshi Mutoh, Takayuki Ustunomiya, Hiroyuki Akashi, Sho Tastuoka
Graduate School, Tokyo Metropolitan University
nmutoh@cc.tmit.ac.jp

***Abstract*- This paper describes a braking control method that is suitable for front-and-rear-wheel-independent-drive-type electric vehicles (FRID EVs). The research on FRID EVs has been accelerated as these vehicles are considered the next-generation electric vehicles (EVs). The braking control proposed in this paper is performed in cooperation with the mechanical braking control and the electric braking control under various load conditions. The proposed cooperative braking control method can realize a stable braking control on low-friction-coefficient (μ) roads; this stable control cannot be realized by the conventional braking control methods. An outstanding braking performance when the proposed braking control method is applied to the FRID EV is demonstrated through simulations and a comparison of the performance of the FRID EV with that of the other EVs. Moreover, the effectiveness of the proposed braking control method is verified through experiments on an official running test course with low-μ roads using a prototype FRID EV with practical specifications.**

I. INTRODUCTION

Triggered by the recent brake issue in hybrid cars [1], interest in the safety of eco-vehicles such as hybrid cars and electric vehicles has increased considerably. The mission of all vehicles is to carry people safely to their destination. In order to achieve this mission, according to the traffic situations or roads conditions, it is necessary to accurately perform a series of vehicles operations until arriving at the destination, that is, basic motions of a car from when it is started to when it is stopped, including acceleration and deceleration operations. Braking operations are directly related to the safety of the vehicle and hence are particularly important. These operations need to be performed appropriately on all types of road surfaces, including very-low-friction-coefficient (μ) roads like icy roads. The brake control plays an important role in maintaining the safety of hybrid cars or EVs, which are due to be used widely from the viewpoint of the regulation of CO_2.

Therefore, from the viewpoint of the safety of vehicles, this paper focuses on the braking control on a low-friction-coefficient (μ) road surface that can induce very dangerous traffic accidents. Currently, many vehicles are equipped with an anti-lock brake system (ABS) in order to prevent wheel lock from occurring at the time of braking; a wheel lock makes it difficult to steer the vehicle. Many researches on ABS have also been carried out [2]-[11]. However, in these researches, load movement [12] generated at the time of braking is hardly focused upon. When the load movement between the front and the rear wheels is not taken into consideration, the braking force applied to each of the four wheels has to be controlled independently according to the road surface [9], [13]. Therefore, in this control, since the braking force generated on the tire of each wheel is different, the attitude control of the vehicle body by steering is required. As a result, it may be very difficult to steer the vehicle.

On the other hand, since the front-and-rear-wheel-independent-drive-type electric vehicles (FRID EVs) focused upon in this study (Fig. 1) have a drive structure that can independently control the driving and the braking forces [14], [15], the load movement produced between the front and the rear wheels at the time of braking can be easily compensated for according to the road surface conditions. Therefore, a braking control method suitable for FRID EVs on a low-μ road is studied here.

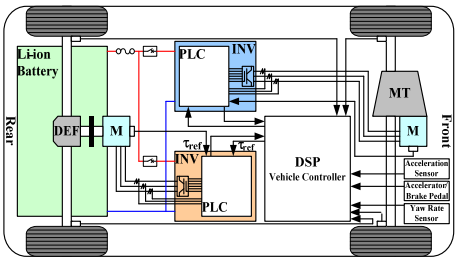

Fig. 1. FRID EV with a drive structure that can compensate for the load movement produced between the front and the rear wheels [14].

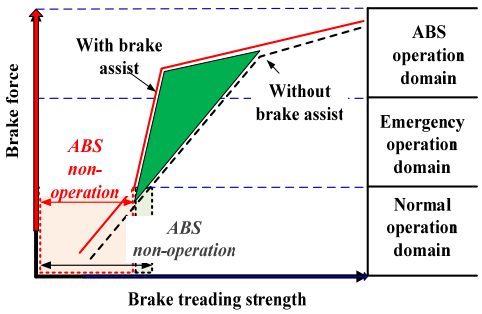

Fig. 2. Operation domain effective in the current anti-lock brake system (ABS) .

Fig. 2 shows the operation domain of the present mechanical ABS based on the oil pressure control [16]. As shown in Fig. 2, there is a big problem that the ABS does not properly operate when the pressure applied on the brake pedal

978-1-4244-8218-4/10/$26.00 ©2010 IEEE

is low. This implies that the ABS does not have a significant effect on a low-μ road as the pressure on the brake pedal is low. In order to deal with this problem, an electrical braking control that can quickly and accurately control the braking force depending on the brake pedal operations even when the pressure applied on the brake pedal is low is performed here. The use of only the electrical brake system cannot generate sufficient brake force; moreover, it is impossible to cope with a situation in which the electrical brake system fails.

Therefore, in order to ensure that a sufficient braking force required for an emergency brake is also generated by the mechanical brake system, a method using which the braking control is performed in cooperation with the electrical brake and the mechanical brake is proposed here.

Here, first, an outstanding electric braking performance of an FRID EV on low-μ roads is clarified through simulations and a comparison of the performance of the FRID EV with that of the current EVs [18] (Figs. 3(b) and (c)). Then, the effectiveness of the proposed braking control method that can effectively perform in cooperation with the mechanical and electric braking controls is verified through experiments on low-μ roads by using a prototype FRID EV with practical specifications and comparing the performance of the proposed braking control with the performance of only the electric braking control.

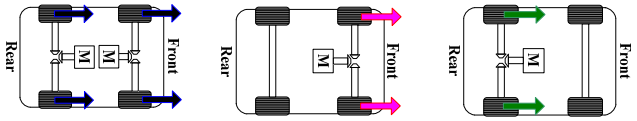

(a) FRID EV proposed by Mutoh et al. [14]

(b) Front wheel motor drive type EV

(c) Rear wheel motor drive type EV

Fig. 3. Drive structure of the FRID EV and current EVs which are used for verifying braking performance during running on low μ-roads.

II. Braking Control Method on Low-μ Roads

A. Braking Control Conditions

In the braking control method proposed here, the structural feature of the FRID EV that can independently control the braking forces F_{B_f} and F_{B_r} (Fig. 4)), which are produced on each tire of the front and the rear wheels, is used. Each of the vehicle dynamics of the front and the rear wheels can be expressed by using the symbols indicated in Fig. 4. The front and the rear wheels have the same independent-drive structures. Therefore, for the sake of simplicity, we focus only on the front wheel; the wheel dynamics can be expressed as

$$J\frac{d\omega_{f\_i}}{dt} = rF_{B\_f} - T_{B\_f}, \tag{1}$$

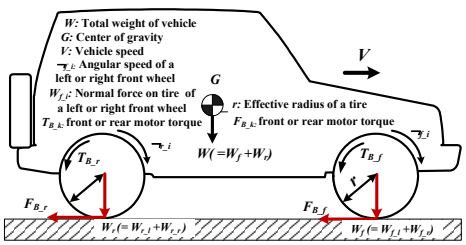

Fig. 4. Wheel dynamics of front-and-rear-independent-drive system during braking.

$$F_{B\_f} = MdV/dt = (W/g)dV/dt, \tag{2}$$

$$F_{B\_f\_\max} = \mu \cdot W. \tag{3}$$

Here, J is the moment of inertia of a front wheel, ω is the rotating angular speed of a front wheel, and $F_{B\_f\_max}$ is the maximum braking force on the tire of the left or right front wheel. The slip ratios of the left and the right front wheels are defined as

$$S_{f\_l} = \frac{V - V_{wf\_l}}{V}, \tag{4}$$

$$S_{f\_r} = \frac{V - V_{wf\_r}}{V}. \tag{5}$$

Here, the torque, which is the output from a front wheel motor, is distributed to each of the left and the right front wheels through a differential gear on the basis of the slip ratio determined from the following calculation:

$$S_f = \max(S_{f\_l}, S_{f\_r}). \tag{6}$$

After finding a wheel with poor stability by using the above equation, we performed the following braking force control so that the stability of the targeted wheel is improved.

$$\frac{d\mu}{dt} \approx -\frac{r}{V}\cdot K \cdot \frac{rF_{B\_f} - T_{B\_f}}{J} \tag{7}$$

$$K = \frac{d\mu}{ds_f} \tag{8}$$

where the condition $dV/dt << d\omega_{f\_i}/dt$ ($i = l$: left wheel, $i = r$: right wheel) is assumed for (6) and J is the moment of inertia of a left or right wheel.

Next, the slope of the μ–slip ratio curve (Fig. 5), i.e., $d\mu/ds$, is focused upon. When K is maintained as a positive constant, the time change of the coefficient of friction increases with an increase in the braking torque T_{B_f} under the condition that the motor torque T_{B_f} is larger than rF_{B_f} ($T_{B\_f} > rF_{B\_f}$). Accordingly, in the linear regions of the μ–slip ratio curve, which are shown in Fig. 5, the wheel speed can be attenuated stably if the braking force control is performed in the range of the slip ratio given by

$$0 \le s_f \le 0.1. \tag{9}$$

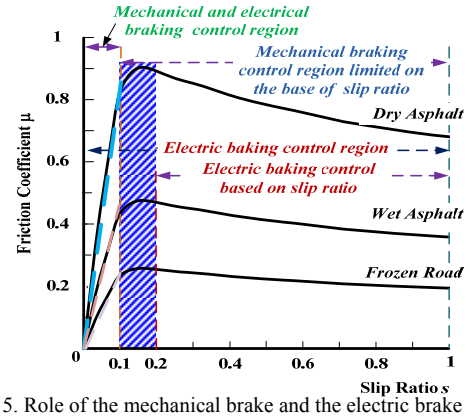

Fig. 5. Role of the mechanical brake and the electric brake according to the slip ratio.

Here, the slip ratio is calculated on the basis of the acceleration α obtained from the acceleration sensor installed at the center of gravity, and the wheel speed that is detected by the pulse encoder attached to each wheel. Here, the vehicle speed $V(t)$ is estimated by using the following equation:

$$V(t) = \int_{t_i}^{t_j} \alpha dt + V(t_i). \tag{10}$$

The above-mentioned integration time (t_i, t_j) is the period until either the accelerator or the brake pedal is released after stepping on the accelerator or the brake pedal; $V(t_i)$ is the wheel speed just before stepping on one of the pedals. This value as detected from a wheel sensor is used as the vehicle speed at the given time and is updated every time the wheel speed is detected as long as both pedals are released.

In the domains of (9), the left and the right front wheel speeds are decreased by the mechanical braking force generated when the oil pressure is applied to a wheel cylinder and the electric braking force that is generated by the front motor.

$$\tau_{mR} = \frac{\tau_B}{1 + T_m \cdot S}, \tag{11}$$

$$\tau_{eR} = \frac{\tau_B}{1 + T_e \cdot S}. \tag{12}$$

Here, τ_B is a value corresponding to the pressure applied on the brake pedal, S is the differential operator, and T_m and T_e are the time constants of the mechanical and the electric brake systems, respectively.

B. Braking Control Procedures

After the above τ_B output from the brake pedal is filtered by (11) and (12), the proposed braking control is performed by using the control procedures (Fig. 6), and the electric-and-mechanical-brake cooperative control system is used for executing these procedures (Fig. 7) on the basis of the obtained τ_{mR} and τ_{eR}. Note that the proposed control is performed in cooperation with the mechanical and electric brakes on the basis of the conditions of the slip ratio and the battery voltage.

Since the electric brake control is based on the regenerative brake, it is performed under the condition $\max(E_{df}, E_{dr}) \leq E_{dmax}$; this condition is satisfied by the inverter input voltages, E_{df} and E_{dr}, of the front and the rear wheels. Here, E_{dmax} is the allowable limit value of the front and the rear inverters and the battery. When this condition is satisfied, the torque limit values, τ_{Bf_max} and τ_{Br_max}, of the front and the rear torque controller are set to zero by

$$\tau_{Bf\_max} \text{ and } \tau_{Br\_max} = 0. \tag{13}$$

When the above-mentioned condition is satisfied, the following processing is performed according to the condition of the slip ratios, s_f and s_r, of the front and the rear wheels.

When the slide ratio is more than 0.2, the limit value of the front wheel or the rear wheel with which the abovementioned condition is satisfied is set to zero by the following procedures:

$$\tau_{Bf\_max} = 0, \text{ if } s_f > 0.2;\ \tau_{Br\_max} = 0, \text{ if } s_r > 0.2\ . \tag{14}$$

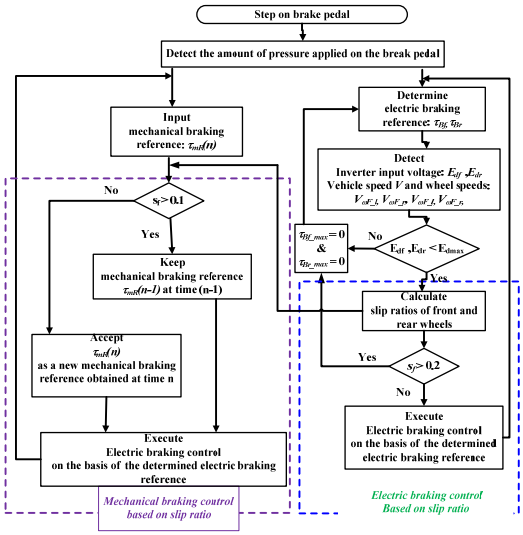

Fig. 6. Procedures for executing the mechanical braking control and the electric braking control.

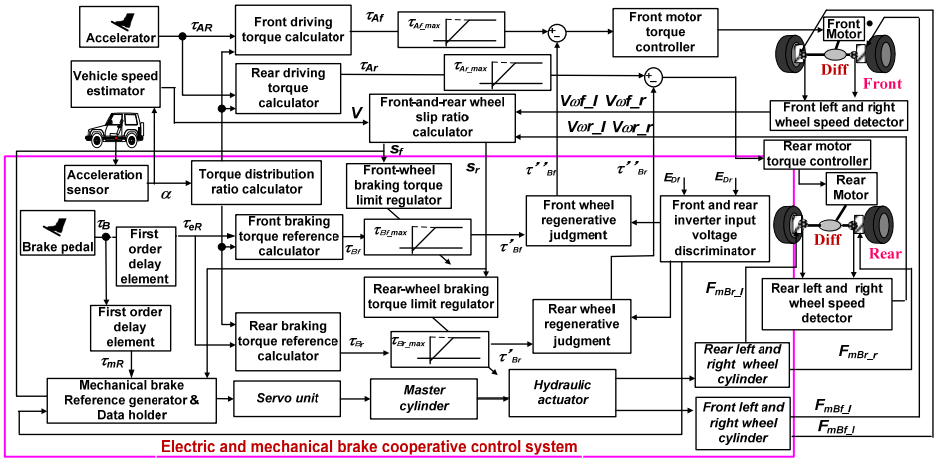

Fig. 7. Block diagram of electric and mechanical brake cooperative control system for executing brake control processing.

When the slip ratio is 0.2 or less, by considering the load movement, we distribute the braking torque to the front and rear wheels by using the following technique. The load movement z shown in Fig. 8 is given by

$$z = \frac{F_{car} \cdot H_{car}}{L_{car}} = \frac{M \cdot \alpha \cdot H_{car}}{L_{car}} \tag{15}$$

where α is the acceleration of the vehicle body as measured by the acceleration sensor installed at the center of gravity, L_{car} is the wheel base, H_{car} is the height of the center of gravity, and M is the vehicle mass. Using the load movement z, we can express the braking forces on the tires of the front and the rear wheels [12] as

$$F_{Bf} = \mu(W_f + z) = \mu(W_f + \frac{F_{car} \cdot H_{car}}{L_{car}}), \tag{16}$$

and

$$F_{Br} = \mu(W_r - z) = \mu(W_r - \frac{F_{car} \cdot H_{car}}{L_{car}}), \tag{17}$$

where W_f and W_r are the front and the rear wheel loads, respectively. In order to estimate the front and the rear braking forces, F_{Bf} and F_{Br}, we use the front and the rear braking torque references, τ_{Bf} and τ_{Br} that are applied to the front and the rear motor torque controller (Fig. 7) and are given by

$$\tau_{Bf} = K_g \cdot R_f \cdot F_{Bf}, \tag{18}$$

and

$$\tau_{Br} = K_g \cdot R_f \cdot F_{Br}. \tag{19}$$

Here, K_g is the torque conversion gain; the torque distribution ratios R_f and R_r are expressed as

$$R_f = \frac{F_{Bf}}{F_{Bf} + F_{Br}} = \frac{\mu(W_f + z)}{\mu(W_f + W_r)} = \frac{\mu(W_f + z)}{\mu \cdot W} = \frac{M_f \cdot g + z}{M \cdot g}, \tag{20}$$

and

$$R_r = 1 - R_f. \tag{21}$$

where g is the acceleration due to gravity and M_f is the front mass that is approximately given by $M/2$.

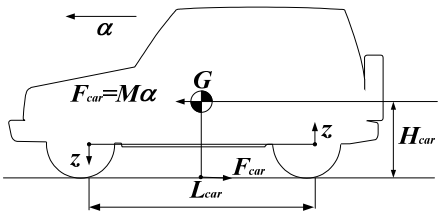

Fig. 8. Load movement produced when the braking force is applied to a vehicle moving on a flat road.

Finally, the mechanical braking processing shown in Fig. 6 is explained. When the slip ratio s, which is determined through processing: max(s_f, s_r) by using the front and the rear slip ratios: s_f(and s_r) given by (4)–(6), is less than 0.1, on the basis of the mechanical braking reference, τ_{mR}, determined from the trod value of the brake pedal, the front and the rear mechanical braking forces F_{mBf} and F_{mBr} required in order to control the disk brake in consideration of the load movement between the front and the rear wheels are determined by using

$$F_{mBf} = K_m \tau_{mB}/2 + z, \tag{22}$$

and

$$F_{mBr} = K_m \tau_{mB}/2 - z, \tag{23}$$

where K_m is the mechanical force conversion gain. Here, the mechanical braking forces F_{mBf_l} and F_{mBf_r} (which are applied to the front-left- and front-right-wheel cylinder), and F_{mBr_l} and F_{mBr_r}, (which are applied to the rear-left- and rear-right-wheel cylinder) are given as $F_{mBf}/2$ (= F_{mBf_r} = F_{mBf_l}) and $F_{mBr}/2$ (= F_{mBr_l} = F_{mBr_r}) from the structure of the used disk brake. When the slip ratio s exceeds 0.1, the same processing as that mentioned above is performed by the mechanical braking torque reference $\tau_{mB}(n-1)$ that is already obtained by the previous processing $(n-1)$ (Fig. 6).

III. Verification of Proposed Braking Control Method

A. Comparison of Braking Performance between FRID EV and Conventional EVs by Simulations

The electric braking performance of the FRID (Fig. 3(a)) is evaluated by a comparison with the braking performance of the current EVs, i.e., the front-wheel motor-drive-type EV

TABLE I.
Specifications of Vehicles Used for Simulations

Item	Value
Vehicle weigh	1900 kg
Overall length	4445 mm
Overall width	1765 mm
Overall height:	1675 mm
Wheel base	2625mm

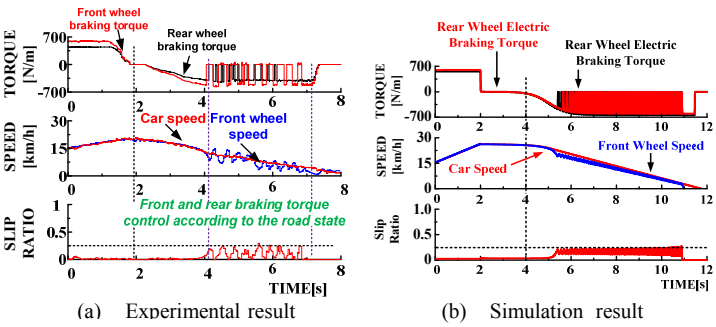

(a) Experimental result (b) Simulation result

Fig. 9. Evaluation of the validity of the simulator when simulations are performed under the almost same conditions as experimental conditions.

(Fig. 3(b)) and the rear-wheel motor-drive-type EV (Fig. 6(c)), which have the same vehicle specifications as those of the prototype FRID EV. The vehicle model simulated using the CarSim software, including Matlab/Simulink is used for a simulator with the specifications given in Table I. First, the effectiveness of the built simulator is evaluated by comparing the experimental results with the simulation results obtained under conditions that are almost the same as the experimental conditions. As shown in Fig. 9, judging from the fact that the simulated results are in good agreement with the experimental results, the built simulator is effective in evaluating the braking control performance of vehicles, including the FRID EV. Fig. 10 shows a comparison of the electric braking performance between the conventional EVs and the FRID EV on low-μ roads (μ = 0.1). The time required for controlling the slip ratio is compared between the front-wheel-and the rear-wheel-drive-type EVs. The compared result shows that the rear-wheel-drive-type EV needs more time to carry out slip control (Figs. 10(a) and (b)). As a result, the latter EV requires more stopping time than the former EV. This is because the load moves to the front wheel side from the rear wheel side and the wheel lock occurs easily on the rear wheel side. This implies that in the case of the rear-wheel-drive-type EV, it is very difficult to obtain a good braking performance on a low-μ road as compared to in the case of the front-wheel-drive EV. On the other hand, the period of the slip control for the FRID EV is shorter than that of the conventional EVs (Fig. 10(c)). Therefore, the stopping time of the FRID EV is the shortest among the three EVs when braking operations are performed on low-μ roads. The braking performance of the driving structure of the FRID EV is verified.

B. Verification of Proposed Braking Control Method by Simulations

First, a comparison of the braking performance between the braking control using the conventional ABS and the electric braking control using the FRID EV on a low-μ road ($\mu = 0.1$) is carried out. The simulation results show that in the case of the ABS (Fig. 11(a)), large fluctuations are seen in the slip ratio due to the bang-bang control and a longer total braking time is needed as compared to in the case of the electric braking control (Fig. 11(b)). Moreover, the simulation results of the braking performance of the proposed braking control method show that since the braking method proposed here can ensure that the changes in the slip ratio remain within a small range, a stable braking control can be realized even on a low-μ road (Fig. 12).

C. Experimental Verification of Proposed Braking Control Method

Finally, the proposed braking control method that controls the brake force by ensuring that the electric braking control cooperates with the mechanical braking control is verified through experiments on very low-μ roads (μ = 0.1) by using a prototype FRID EV with practical specifications. The experiments were performed in comparison with the use of only the electric braking control. When only the electric braking control was performed, Fig. 13 shows that the FRID EV stopped, resulting in a fluctuation of the slip ratio (Fig. 13(b)). However, when the proposed braking control was performed, the change in the slip ratio was hardly observed and the FRID EV stopped smoothly (Fig. 13(c)).

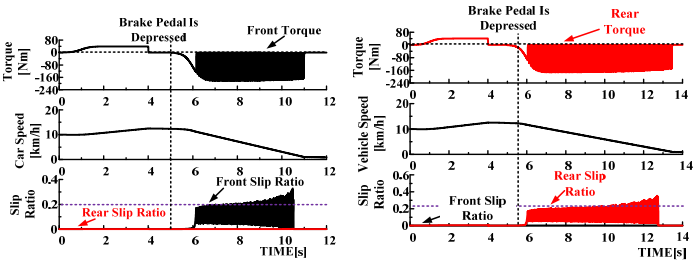

(a) Front wheel motor drive type EV

(b) Rear wheel motor drive type EV

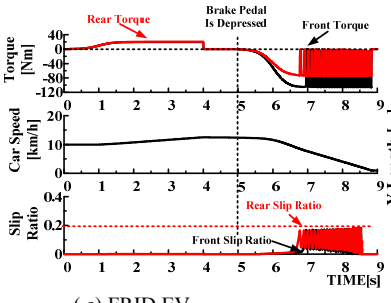

(c) FRID EV

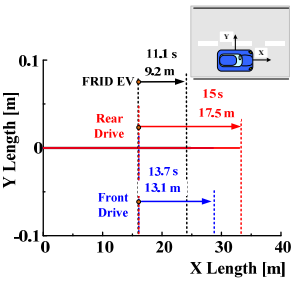

(d) Differences between the braking time and distance

Fig.10. Comparison of electric braking performance between the conventional EVs and the FRID EV on low-μ roads (μ = 0. 1).

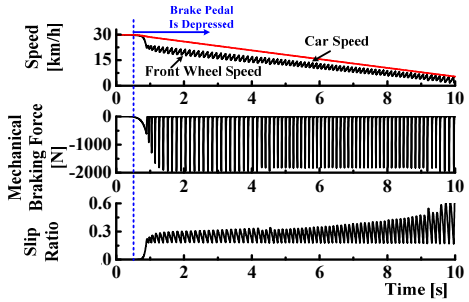

(a) When the conventional braking control using ABS is performed.

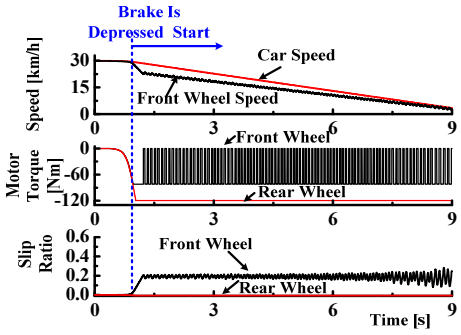

(b) When the electric braking control using FRID EV is performed

Fig. 11. Stability of the electric-brake-type FRID EV when the brake operation is carried out at low vehicle speeds on low-μ roads as compared to that of a conventional ABS.

The proposed braking control method that can sufficiently pull out the structural feature of the FRID EV that the front and rear drive systems are mutually independently formed is a function indispensable to the next-generation EV.

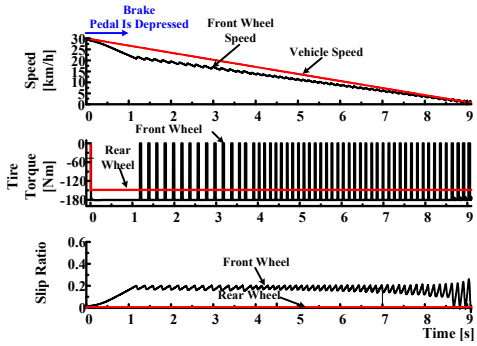

(a) When only the electric braking control is performed.

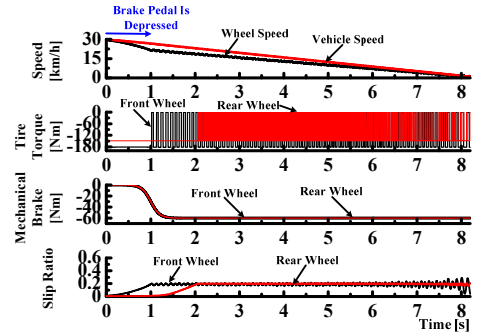

(b) When the proposed braking control is performed.

Fig.12. Verification of the performance of the proposed braking control on a flat road with a friction coefficient of 0.1 as compared to the performance when only the electric braking control was used.

(a) Photograph of the FRID EV on a test course with a low friction coefficient

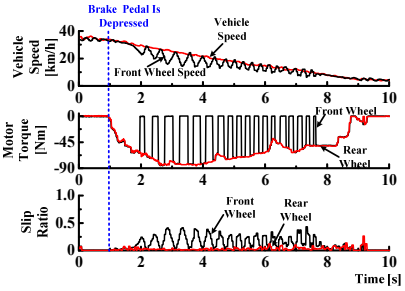

(b) When only electric braking control was performed.

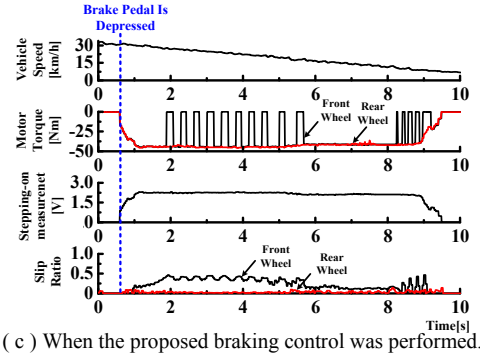

(c) When the proposed braking control was performed.

Fig. 13. Experimental verification of the braking performance when the proposed braking control method was applied to the FRID EV.

V. Conclusion

In this paper, we proposed a braking control method indispensable to the stable and safe running of vehicles on low-μ roads. The effectiveness of the braking control method was verified through simulations and experiments. Through the simulations, it was clarified that the braking performance of the FRID EV was superior to that of the present EVs and the ABS. Moreover, experiments showed that the FRID EV to which the proposed braking control was applied could also run stably and smoothly on low-μ roads.

It is expected that the proposed braking control will become an important function of the FRID EV in which safety and running performance are compatible.

References

[1] "Sorting out hybrid brake issue: safety issue or a different feel?" http://www.hybridcars.com/safety/sorting-out-hybrid-brake-issue-safety-issue-or-different-feel-26604.html, Published Feb. 5, 2010.

[2] C. Mi, H. Lin, and Y. Zhang, "Iterative learning control of antilock braking of electric and hybrid vehicles," *IEEE Trans. on Vehicular Tech*. vol. 54, no. 2, pp. 486-494, 2005.

[3] T. Shim, S. Chang, and S. Lee, "Investigation of sliding-surface design on the performance of sliding mode controller in antilock braking systems," *IEEE Trans. on Vehicular Tech*. vol. 57, no. 2, pp. 747-759, 2008.

[4] E. Kayacan, Y. Oniz, and O. Kaynak, "A grey system modeling approach for siding-mode control of antilock braking system," *IEEE Trans. on Industrial Electro*. vol. 56, no. 8, pp. 3244-3252, 2009.

[5] S.B. Choi, "Antilock brake system with a continuous wheel slip control to maximize the braking performance and the ride quality," *IEEE Trans. on Control Sys. Tech.*, vol. 16, no. 5, pp. 996-1003, 2008.

[6] Y. Mao, Y. Zheng, Y. Jing, G.M. Dimirovski, and S. Hang, "An LMI approach to slip ratio control of vehicle antilock braking systems," *2009 American Control Conference*, St. Louis, MO, June 10-12, 2009.

[7] G. Celentano, R. Iervolino, S. Porreca, and V. Fontana, "Car brake system modeling for longitudinal control design," *IEEE CCA 2003,* vol. 1, pp. 25-30, June 23-25, 2003.

[8] S. Anwar, "An anti-lock braking control system for a hybrid electromagnetic/electrohydraulic brake-by-wire system," *American Control Conference*, 2004, vol. 3, pp. 2699-2704, June 30-July 2, 2004.

[9] J. Wang, C. Song, and L. Jin, "A composite ABS control method for EV with four independently driving wheels," *ISA* 2010, pp. 1-4, May 22-23, 2010.

[10] W.K. Lennon and K.M. Passino, "Intelligent control for brake systems," *IEEE Trans. on Control Sys. Tech.*, vol. 7, no. 2, pp.188- 202, 1999.

[11] C. Liang, S. Wanfeng, Y. Liang, Z. Yongsheng, O. Yang, W. Wenruo, L. Minghui, and L. Jun, "Integrative control strategy of regenerative and hydraulic braking for hybrid electric car," *IEEE VPPC2008*, Dearborn, MI , pp.1091-1098, Sept. 7-10, 2009.

[12] N. Mutoh, Y. Hayano, H. Yahagi, and K. Takita, "Electric braking control methods for electric vehicles with independently driven front and rear wheels," *IEEE Trans. on Industrial Electro*., vol. 54, no. 2, pp. 1168-1176, 2007.

[13] F. Tahami, R. Kazemi, and S. Farhanghi, "A novel driver assist stability system for all-wheel-drive electric vehicles," *IEEE Trans. on Vehicular Tech.*, vol. 52, no. 3, pp. 683-692, 2003.

[14] N. Mutoh *et al.*, "Electric vehicle drive system and drive method," US Patent 5549172.

[15] N. Mutoh, T. Kazama, and K. Takita, "Driving characteristics of an electric vehicle system with independently driven front and rear wheels," *IEEE Trans. on Industrial Electro.* vol. 5 3, no. 3, pp. 803-813, 2006.

[16] Regarding ABS: http://www.mitsubishi-motors.com/jp/spirit/technology/library/abs.html.

[17] For example: i-MiEV (Mitsubishi Motors): http://www.ev-life.com/.